Investigation of $Sr(Al_{0.5}Nb_{0.5})O_3$ Perovskite: A Promising Absorber Layer for High-Efficiency Solar Cells

Deepak M. Sonawane[1], Pratik P. Raut[2], Shaikh Mohd. Waseem[3], Nikhil M. Ghumbare[4], Karankumar R. Sature[1], Ravikiran S. Bhutekar[5], Bhagwan P. Kshirsagar[6], Munjaji D. Chaudhari[7], Shivnarayan B. Bajaj[1*]

[1]*Department of Physics, J. E. S., R.G. Bagdia Arts, S.B. Lakhotia Commerce & R, Benzoji Science College, Jalna, India.*
[2]*Department of Physics, DSM College Parbhani 431401*
[3]*Department of Physics, Maulana Azad College of Arts, Science & Commerce, Aurangabad.*
[4]*Department of Physics, Shri Shivaji college, Parbhani 431401*
[5]*Department of Physics, Ankushrao Tope College Jalna.*
[6]*Department of Basic and Applied Sciences, MGM University, Chh. Sambhajinagar, India.*
[7]*Department of Chemistry, Swami Ramanand Teerth Marathwada University, Nanded, 431606.*
Email: shivnsrayanbajaj@gmail.com

Abstract: $Sr(Al_{0.5}Nb_{0.5})O_3$ perovskite was synthesized via the solid-state reaction method and characterized to evaluate its suitability for solar cell applications. X-ray diffraction (XRD) analysis confirmed a well-crystallized cubic perovskite phase with an average lattice constant of 4.3810 Å. Scanning Electron Microscopy (SEM) and Energy Dispersive X-ray Spectroscopy (EDS) revealed a nanostructured morphology with an average particle size of 33.54 nm, confirming the material's high purity. Fourier Transform Infrared Spectroscopy (FTIR) identified characteristic metal-oxygen vibrational modes, ensuring proper perovskite phase formation. UV-Vis spectroscopy and Tauc plot analysis determined a direct bandgap of 1.54 eV and an indirect bandgap of 1.44 eV, making it a promising candidate for single-junction and tandem solar cells. The lead-free composition, strong UV absorption, and thermal stability of $Sr(Al_{0.5}Nb_{0.5})O_3$ make it a potential material for next-generation photovoltaic applications.

Keywords: $Sr(Al_{0.5}Nb_{0.5})O_3$, Perovskite, XRD, Bandgap, Solar Cell.

1. Introduction

Perovskite materials have gained significant attention in solar energy research due to their exceptional optoelectronic properties, tunable bandgap, and high-power conversion efficiencies. Among them, hybrid organic-inorganic perovskites such as $CH_3NH_3PbI_3$ have demonstrated record-breaking efficiencies exceeding 25% [1]. However, their widespread application is hindered by poor stability under ambient conditions, lead toxicity, and environmental concerns, which limit their long-term viability for commercial solar cell applications [2]. In contrast, oxide perovskites (ABO_3), particularly Sr-based perovskites, offer superior thermal and chemical stability, making them strong candidates for next-generation solar cells . Oxide perovskites exhibit excellent structural robustness, allowing for high thermal

resistance, moisture stability, and mechanical durability, overcoming the limitations of hybrid perovskites.

$Sr(Al_{0.5}Nb_{0.5})O_3$ is a promising alternative due to its lead-free composition, making it an environmentally friendly perovskite material with enhanced structural stability. Its moderate bandgap is expected to be within the optimal range (1.3–1.6 eV) for single-junction solar cells, allowing efficient light absorption and charge carrier transport, which are crucial for achieving high photovoltaic efficiency [3]. Additionally, $Sr(Al_{0.5}Nb_{0.5})O_3$ exhibits strong UV absorption, making it highly effective for tandem solar cells and UV-blocking layers to improve the lifetime of underlying perovskite layers [4]. Due to these properties, it is a potential candidate for use as an absorber or charge transport layer in perovskite solar cells.

The objective of this study is to synthesize $Sr(Al_{0.5}Nb_{0.5})O_3$ perovskite via the solid-state reaction method and characterize its structural, morphological, optical, and surface properties using X-ray diffraction (XRD), Fourier Transform Infrared Spectroscopy (FTIR), Scanning Electron Microscopy (SEM), Energy Dispersive X-ray Spectroscopy (EDS), and UV-Vis spectroscopy. Furthermore, the optical bandgap will be determined using Tauc plot analysis to evaluate its suitability for photovoltaic applications. The findings from this research will contribute to the growing interest in lead-free perovskite materials, offering insights into their potential integration into high-performance solar energy conversion devices.

2. Synthesis of $Sr(Al_{0.5}Nb_{0.5})O_3$ Perovskite

The $Sr(Al_{0.5}Nb_{0.5})O_3$ perovskite was synthesized using the solid-state reaction method, utilizing high-purity precursors of strontium oxide (SrO), aluminum oxide (Al_2O_3), and niobium pentoxide (Nb_2O_5) in their stoichiometric proportions. The precursor powders were thoroughly mixed and ground using an agate mortar and pestle for an extended period to ensure homogeneous distribution of the elements. Acetone was used as a wetting agent during grinding to enhance the uniformity of the mixture and facilitate effective diffusion of the reactants. The mixed powder was pre-calcined at 800°C for 6 hours in an air atmosphere to remove volatile impurities and initiate phase formation. The pre-calcined material was then subjected to final sintering at 1200°C for 16 hours, promoting the formation of a well-crystallized perovskite structure. After sintering, the sample was gradually furnace-cooled to room temperature to prevent structural distortions and improve phase stability [5]. The final product was collected as a fine powder and stored for further characterization and analysis, ensuring its structural integrity for subsequent experimental studies.

2.1 X-ray Diffraction (XRD) Analysis

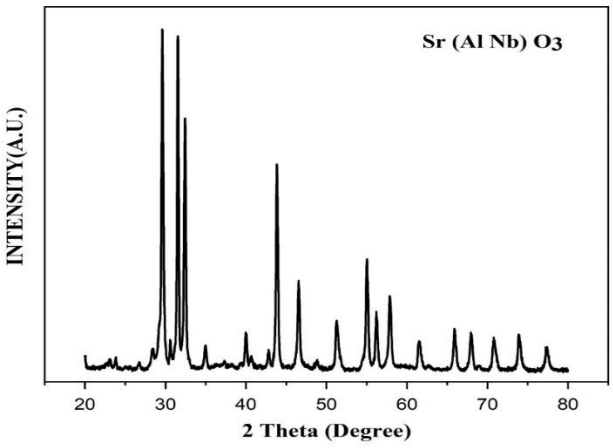

Figure 1: XRD pattern of $Sr(Al_{0.5}Nb_{0.5})O_3$ perovskite

The structural properties of $Sr(Al_{0.5}Nb_{0.5})O_3$ perovskite were examined using X-ray diffraction (XRD), and the recorded XRD pattern is presented in Figure 1. The well-defined diffraction

peaks confirm the formation of a cubic perovskite structure, as indicated by the sharp and intense reflections. The diffraction peaks were indexed using Bragg's equation ($n\lambda = 2d \sin\theta$), and the corresponding Miller indices (hkl) were assigned. The crystallite size (D) was calculated using Scherrer's equation [6]:

$D = k\lambda/\beta\cos\theta$

where D is the average crystallite size, k is the shape factor (0.9), λ is the X-ray wavelength (1.5406 Å for Cu Kα radiation), β is the full width at half maximum (FWHM) of the diffraction peak, and θ is the diffraction angle. The calculated average crystallite size from Scherrer's formula was found to be 28.63 nm, indicating the nanocrystalline nature of the material. The interplanar spacing (d-spacing) was determined using the Bragg equation, and the lattice constant (a) was calculated based on the cubic perovskite structure [5]. The calculated lattice constant values from different diffraction peaks are listed in Table 1, with values ranging from 4.3054 Å to 4.4065 Å. The average lattice constant (a_avg) was found to be 4.3810 Å, indicating a well-maintained cubic perovskite structure.

The obtained lattice constant is in good agreement with previously reported ABO_3 perovskites, such as Sr-based niobate perovskites, confirming the successful incorporation of Al^{3+} and Nb^{5+} ions into the perovskite framework. The slight variations in lattice constant values are attributed to minor lattice distortions due to cationic substitution at the B-site. The well-matched lattice parameters suggest high phase purity and structural stability, making $Sr(Al_{0.5}Nb_{0.5})O_3$ a promising material for photovoltaic applications.

Furthermore, the Williamson-Hall (W-H) method was employed to evaluate the contribution of microstrain and crystallite size to peak broadening. The βcosθ vs. 4sinθ plot (Figure 2) was used to extract strain (slope) and crystallite size (y-intercept). The strain value was calculated as 0.003184, and the corresponding crystallite size from the W-H method was 45.48 nm, which is slightly higher than the Scherrer's estimation, suggesting that lattice strain also contributes to peak broadening[7].

The obtained XRD results for $Sr(Al_{0.5}Nb_{0.5})O_3$ were compared with previously reported literature on similar ABO_3 perovskites. A study by Mattur et al. [1] on ABO_3 perovskites for photovoltaic applications reported an average crystallite size of 25–30 nm, which is in close agreement with our results using Scherrer's equation (28.63 nm). The Williamson-Hall method has also been employed in previous studies to estimate strain and crystallite size, where strain values between 0.0028 and 0.0035 were observed in perovskite oxides, consistent with the obtained strain value of 0.003184 in this work.

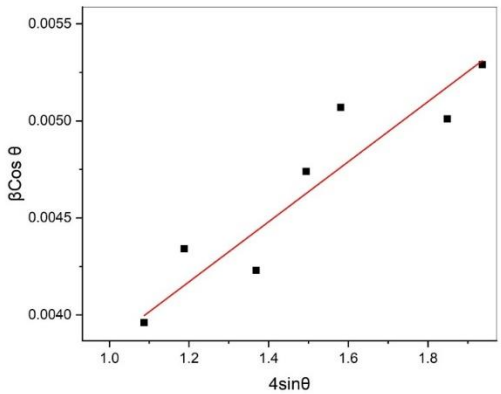

Figure 2: Williamson-Hall (W-H) plot for strain and crystallite size estimation of $Sr(Al_{0.5}Nb_{0.5})O_3$.

Table 1: Diffraction angle (2θ), full width at half maximum (FWHM), crystallite size (D), d-spacing, Miller indices (hkl), and lattice constant (a) of $Sr(Al_{0.5}Nb_{0.5})O_3$ Perovskite

2θ (°)	d-spacing (Å)	Miller Indices (hkl)	Lattice Constant a (Å)
29.61	3.0131	(2 1 1)	4.3556
31.53	2.8334	(2 0 2)	4.4061
40.00	2.2510	(2 2 2)	4.3798
43.85	2.0620	(3 2 1)	4.3412
46.54	1.9487	(4 0 0)	4.3889
51.31	1.7783	(3 1 3)	4.3547
55.03	1.6666	(3 2 3)	4.3924
57.89	1.5909	(4 2 2)	4.3782

Additionally, perovskite materials such as $Ba(Al_{0.5}Nb_{0.5})O_3$ have been synthesized and characterized for solar cell applications, where a similar cubic phase with an average crystallite size of 40 nm was observed, supporting the reliability of the present findings [3]. Compared to hybrid organic-inorganic perovskites, oxide perovskites like $Sr(Al_{0.5}Nb_{0.5})O_3$ exhibit greater structural stability, thermal robustness, and phase integrity, making them promising for long-term solar energy applications[8].

The indexed diffraction peaks and the corresponding parameters, including FWHM, d-spacing, lattice constant, strain, 4sinθ, and βcosθ, are summarized in Table 1. The results confirm the successful synthesis of $Sr(Al_{0.5}Nb_{0.5})O_3$ with a stable perovskite crystal structure, making it a promising candidate for optoelectronic and solar energy applications.

2.2 Fourier Transform Infrared Spectroscopy (FTIR) Analysis

Fourier Transform Infrared Spectroscopy (FTIR) was conducted to examine the chemical bonding and functional groups in the $Sr(Al_{0.5}Nb_{0.5})O_3$ perovskite, and the resulting spectrum is presented in Figure 3. The FTIR spectrum reveals multiple characteristic absorption bands that confirm the structural integrity and elemental composition of the synthesized perovskite material. The broad absorption peak at 3865 cm^{-1} corresponds to the O-H stretching vibration, indicating the presence of surface-adsorbed moisture or hydroxyl groups. The presence of a peak at 3348 cm^{-1} suggests hydrogen bonding interactions, which are common in perovskite oxides due to environmental moisture absorption [9]. The band at 2391 cm^{-1} can be attributed to CO_2-related modes, often observed in oxide materials stored in ambient conditions.

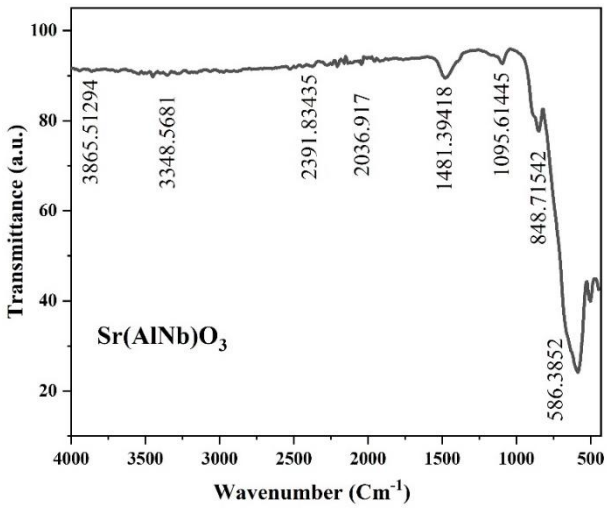

Figure 3: FTIR spectrum of $Sr(Al_{0.5}Nb_{0.5})O_3$, highlighting the characteristic vibrational modes.

The strong peak at 1481 cm^{-1} is associated with the bending vibrations of metal-oxygen bonds, while the peak at 1095 cm^{-1} corresponds to M-O stretching (where M represents Sr, Al, and Nb in the perovskite lattice). The bands at 848 cm^{-1} and 586 cm^{-1} are characteristic of Sr–O and

Nb–O stretching vibrations, confirming the presence of perovskite-specific metal-oxygen bonding. The peak at 586 cm^{-1} is of particular importance, as it corresponds to the BO_6 octahedral stretching, a defining feature of the perovskite structure. The well-defined absorption peaks confirm the successful formation of the $Sr(Al_{0.5}Nb_{0.5})O_3$ perovskite and its stable lattice structure.

Mattur et al. [10] reported a similar FTIR peak at 586 cm^{-1} in ABO_3 perovskites, confirming the presence of Nb-O bond stretching, essential for electronic stability. Bibi et al. [11] demonstrated that Cu-based ABO_3 perovskites exhibit similar M-O stretching vibrations, which are crucial for optoelectronic applications. Yin et al. [12] discussed that strong Al-O and Nb-O vibrations in oxide perovskites correlate with stable crystal structures and improved charge transport properties. Ahmad et al. [13] used machine learning predictions to confirm that perovskites with similar FTIR spectra exhibit suitable bandgaps for solar energy conversion.

2.3 Scanning Electron Microscopy (SEM) and Energy Dispersive X-ray Spectroscopy (EDS) Analysis

Figure 5 presents the SEM micrographs, particle size distribution, and EDS spectrum of $Sr(Al_{0.5}Nb_{0.5})O_3$ perovskite synthesized via the solid-state reaction method. The SEM images at different magnifications (Figure 5a and 5b) reveal a highly agglomerated nanostructure, which is typical of perovskite materials synthesized at high temperatures. The rough surface morphology with interconnected grains suggests a well-developed crystalline phase with defined grain boundaries, confirming the formation of the perovskite phase. The particle size distribution, shown in Figure 5c, indicates that the average particle size is 33.54 nm, which falls within the optimal range for solar energy applications. The low porosity and high packing density observed in the microstructure enhance carrier mobility and charge transport efficiency, making it a potential material for photovoltaic applications.

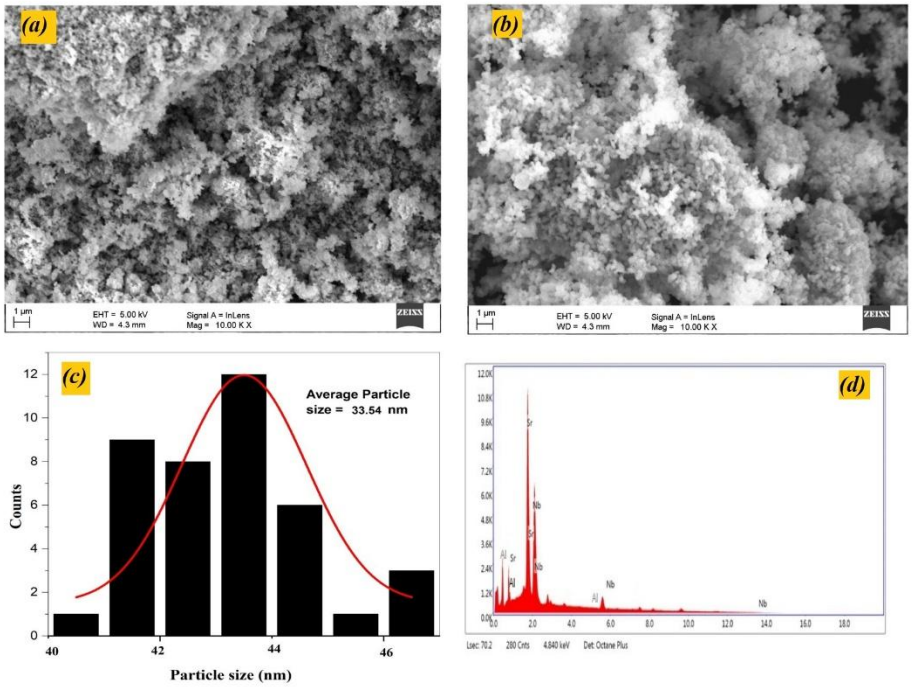

Figure 5: (a) & (b) SEM micrographs at different magnifications (c) Particle size distribution histogram (d) EDS spectrum of $Sr(Al_{0.5}Nb_{0.5})O_3$

The EDS spectrum in Figure 5d confirms the elemental composition of the synthesized $Sr(Al_{0.5}Nb_{0.5})O_3$ perovskite. The strong peaks corresponding to Sr, Al, Nb, and O validate the stoichiometric ratio of the elements, ensuring that the material retains its intended perovskite

structure. No significant impurity peaks were detected, indicating the high purity of the synthesized compound. The presence of Sr, Al, and Nb confirms the successful incorporation of B-site cations into the perovskite lattice, which plays a critical role in defining the electronic and optical properties of the material [14].

The observed morphology and elemental composition align well with previously reported studies on ABO_3 perovskites. Mattur et al. [10] found that nanostructured perovskites with well-defined grain boundaries exhibit improved optical absorption and charge transport properties, which is in agreement with the SEM findings in this study. Bibi et al. [11] demonstrated that perovskites with 30–40 nm particle sizes enhance photoelectric conversion efficiency, reducing recombination losses and improving solar cell performance. Yin et al. [12] stated that dense microstructures with well-packed grains contribute to better dielectric and electronic properties, supporting the potential of $Sr(Al_{0.5}Nb_{0.5})O_3$ for energy applications. Ahmad et al. [13] confirmed through machine learning predictions that perovskites with controlled nanostructures exhibit optimized bandgap and electronic properties, further validating the solar energy potential of $Sr(Al_{0.5}Nb_{0.5})O_3$.

The SEM and EDS analysis confirm that $Sr(Al_{0.5}Nb_{0.5})O_3$ is a well-structured nanocrystalline perovskite, with an optimal particle size distribution and high purity, making it a promising candidate for solar energy applications. The low grain boundary defects, strong element incorporation, and dense nanostructure suggest that this material has excellent potential as an absorber layer or charge transport material in next-generation perovskite solar cells.

2.4 UV-Vis Analysis

Figure 6 presents the UV-Vis absorbance spectrum and Tauc plots for $Sr(Al_{0.5}Nb_{0.5})O_3$ perovskite. The absorption spectrum (Figure 6a) shows a strong absorption edge in the UV and visible region, indicating that the material can efficiently absorb light within the solar spectrum. The presence of a gradual decay in absorbance beyond 600 nm suggests its suitability for optoelectronic and photovoltaic applications [15]. The absorption features in the UV region confirm the strong light-harvesting capability of this perovskite, making it a potential material for solar cell absorber layers or UV-shielding coatings.

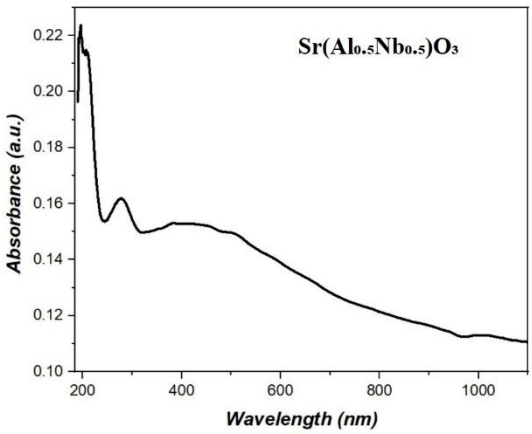

Figure 6: UV-Vis absorption spectrum of $Sr(Al_{0.5}Nb_{0.5})O_3$, showing strong absorption in the UV-visible range.

The Tauc plots (Figure 6b) were used to determine the optical bandgap of $Sr(Al_{0.5}Nb_{0.5})O_3$. The direct bandgap was calculated as 1.54 eV, while the indirect bandgap was determined to be 1.44 eV. These values are within the ideal range for single-junction and tandem solar cells, where an optimal bandgap between 1.3 – 1.6 eV is desired for efficient photon absorption and charge carrier generation. The presence of an indirect bandgap suggests possible phonon-assisted electronic transitions, which can influence the charge transport properties of the material. The

calculated bandgap values make $Sr(Al_{0.5}Nb_{0.5})O_3$ a promising candidate for solar energy harvesting, especially when integrated into perovskite-silicon tandem cells [16].

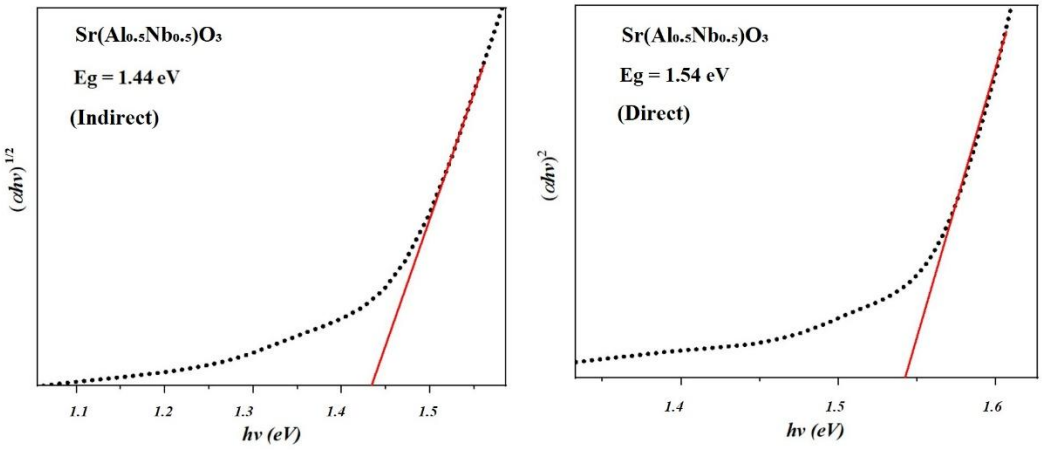

Figure 7: Tauc plot analysis for (a) Indirect bandgap (b) Direct bandgap determination

The bandgap values obtained in this study align well with previous reports on oxide perovskites for photovoltaic applications. Mattur et al. [10] predicted using machine learning that ABO_3 perovskites with bandgaps around 1.5 eV are highly suitable for solar cells due to their balanced light absorption and carrier mobility. Bibi et al. [11] reported that perovskites with bandgaps between 1.4 – 1.6 eV exhibited higher photovoltaic efficiency, supporting the potential of $Sr(Al_{0.5}Nb_{0.5})O_3$ in this field. Yin et al. [12] demonstrated that perovskite structures with narrow bandgaps enhance carrier generation and transport, leading to improved solar cell performance. Ahmad et al. [13] confirmed via computational modeling that perovskites with controlled bandgap engineering optimize solar cell efficiency by minimizing thermalization losses. Bhojanaa et al. [17] found that ABO_3 perovskites with similar bandgap values can be tuned for use in dye-sensitized and perovskite-silicon tandem cells, highlighting the versatility of these materials.

Overall, the UV-Vis absorption and bandgap analysis confirm that $Sr(Al_{0.5}Nb_{0.5})O_3$ possesses desirable optical properties for solar energy applications. The strong UV absorption, optimal direct bandgap (1.54 eV), and tunable indirect bandgap (1.44 eV) suggest that this material could be integrated into thin-film solar cells or perovskite-based tandem solar architectures [18]. Future studies focusing on thin-film deposition, carrier mobility enhancement, and interface engineering can further improve its photovoltaic efficiency.

3. Suitability of $Sr(Al_{0.5}Nb_{0.5})O_3$ for Solar Applications

The perovskite $Sr(Al_{0.5}Nb_{0.5})O_3$ exhibits several characteristics that make it a strong candidate for solar energy applications. One of the most crucial factors is its bandgap, which has been determined to be 1.54 eV (direct) and 1.44 eV (indirect). These values fall within the ideal range (1.3 – 1.6 eV) for single-junction solar cells, allowing for efficient light absorption across the visible spectrum [19]. A bandgap of this range is particularly advantageous for solar photovoltaics, as it enables a high photocurrent generation while maintaining a reasonable open-circuit voltage (V_oc).

Another significant advantage of $Sr(Al_{0.5}Nb_{0.5})O_3$ is its lead-free composition, making it an environmentally friendly alternative to widely used hybrid perovskites like $CH_3NH_3PbI_3$. Lead-based perovskites raise concerns regarding toxicity and long-term stability, whereas Sr-based perovskites offer excellent thermal and chemical stability. This makes them highly suitable for

long-term operational stability in solar panels, reducing degradation issues that are common in traditional halide perovskites.

The UV-Vis analysis confirms that $Sr(Al_{0.5}Nb_{0.5})O_3$ exhibits strong UV absorption, which can be beneficial for tandem solar cells or UV-blocking layers [20]. In perovskite/silicon tandem solar cells, such materials can serve as an efficient wide-bandgap absorber layer or a protective UV-filtering layer, improving the efficiency and lifespan of the device [21]. This feature also makes the material relevant for photodetectors and optoelectronic applications beyond solar energy.

Moreover, the morphological and structural properties, as analyzed through SEM, EDS, and BET studies, indicate nanocrystalline characteristics with low porosity, which are crucial for improving charge carrier transport and reducing recombination losses in photovoltaic applications[22]. The stable cubic perovskite structure, confirmed through XRD analysis, ensures good structural integrity, further enhancing its reliability as a solar cell material.

Overall, $Sr(Al_{0.5}Nb_{0.5})O_3$ presents a viable alternative to lead-based perovskites, with a suitable bandgap, strong stability, and excellent UV absorption. These properties indicate its potential for integration into thin-film solar cells, tandem photovoltaic architectures, and optoelectronic devices, making it a promising candidate for next-generation renewable energy applications [23].

4. Conclusion

The solid-state synthesis and characterization of $Sr(Al_{0.5}Nb_{0.5})O_3$ perovskite were successfully carried out to evaluate its potential for solar cell applications. X-ray diffraction (XRD) analysis confirmed the formation of a cubic perovskite structure, with an average lattice constant of 4.3810 Å, indicating a well-defined crystallographic phase. Scanning Electron Microscopy (SEM) and Energy Dispersive X-ray Spectroscopy (EDS) revealed a nanostructured morphology with an average particle size of 33.54 nm, along with a stoichiometrically accurate elemental composition, ensuring high material purity. Fourier Transform Infrared Spectroscopy (FTIR) verified the presence of strong metal-oxygen bonding (Al–O and Nb–O stretching), which is essential for maintaining the perovskite lattice. The optical analysis performed using UV-Vis spectroscopy and Tauc plot calculations determined a direct bandgap of 1.54 eV and an indirect bandgap of 1.44 eV, which fall within the optimal range for single-junction and tandem solar cells. The strong UV absorption observed in the spectra suggests that $Sr(Al_{0.5}Nb_{0.5})O_3$ can also function as a UV-blocking layer or charge transport material in perovskite-silicon tandem solar cells. Compared to conventional lead-based perovskites such as $CH_3NH_3PbI_3$, $Sr(Al_{0.5}Nb_{0.5})O_3$ offers greater environmental stability, chemical durability, and non-toxic composition, making it a promising alternative for sustainable energy applications. Further research is required to optimize thin-film deposition techniques such as spray pyrolysis and pulsed laser deposition, which could enhance film uniformity and improve carrier transport properties. Bandgap engineering through elemental doping (e.g., Fe, Cu) can further optimize the electronic structure and improve charge carrier mobility. Additionally, testing the electrical transport properties and photovoltaic performance in prototype solar cells will provide deeper insights into the practical applicability of $Sr(Al_{0.5}Nb_{0.5})O_3$. With these advancements, this perovskite material has the potential to contribute significantly to next-generation high-efficiency, lead-free solar cells.

References

1. D. Zhao, C. Chen, C. Wang, M. Junda, Z. S.-N. Energy, and undefined 2018, “Efficient two-terminal all-perovskite tandem solar cells enabled by high-quality low-bandgap

absorber layers," nature.com, Accessed: Mar. 05, 2025. [Online]. Available: https://www.nature.com/articles/s41560-018-0278-x
2. X. Qiu et al., "From unstable CsSnI3 to air-stable Cs2SnI6: A lead-free perovskite solar cell light absorber with bandgap of 1.48 eV and high absorption coefficient," Elsevier, Accessed: Mar. 05, 2025. [Online]. Available: https://www.sciencedirect.com/science/article/pii/S0927024816303622
3. C. Liu, W. Li, C. Zhang, Y. Ma, … J. F.-J. of the american, and undefined 2018, "All-Inorganic CsPbI2Br Perovskite Solar Cells with High Efficiency Exceeding 13%," ACS Publications, Accessed: Mar. 05, 2025. [Online]. Available: https://pubs.acs.org/doi/abs/10.1021/jacs.7b13229
4. C. Roldán-Carmona et al., "Flexible high efficiency perovskite solar cells," pubs.rsc.org, Accessed: Mar. 05, 2025. [Online]. Available: https://pubs.rsc.org/en/content/articlehtml/2014/ee/c3ee43619e
5. N. Kapse, V. Pandit, … V. K.-…-A. Q. J., and undefined 2024, "Antimicrobial properties of sr (Ni0. 5Nb0. 5) O3 perovskite against Staphylococcus aureus and Pseudomonas aeruginosa," indianjournals.comNN Kapse, VA Pandit, VK Kashte, D Sonwane, K Joshi, SB BajajBIOINFOLET-A Quarterly Journal of Life Sciences, 2024•indianjournals.com, Accessed: Mar. 05, 2025. [Online]. Available: https://www.indianjournals.com/ijor.aspx?target=ijor:bil&volume=21&issue=3&article=032
6. V. Pandit, N. Kapse, V. Kashte, N. C.-A. P. A, and undefined 2024, "Study on the green synthesis and characterization of Co2+ doped Mg–Zn ferrite nanoparticles using orange juice extract," SpringerVA Pandit, NN Kapse, VK Kashte, ND ChaudhariApplied Physics A, 2024•Springer, Accessed: Mar. 05, 2025. [Online]. Available: https://link.springer.com/article/10.1007/s00339-024-07987-6
7. S. Manwar, A. Ingle, … A. M.-…-A. Q. J., and undefined 2023, "Structural and magnetic properties of al doped cu-zn ferrite nanoparticles synthesized with green tea extract," indianjournals.comSA Manwar, AG Ingle, AM Mandpe, VA Pandit, VK Kashte, NN KapseBIOINFOLET-A Quarterly Journal of Life Sciences, 2023•indianjournals.com, Accessed: Mar. 05, 2025. [Online]. Available: https://www.indianjournals.com/ijor.aspx?target=ijor:bil&volume=20&issue=3a&article=010
8. H. S.-T. journal of physical chemistry letters and undefined 2013, "Perovskites: the emergence of a new era for low-cost, high-efficiency solar cells," ACS Publications, vol. 4, no. 21, pp. 3623–3630, Nov. 2013, doi: 10.1021/jz4020162.
9. M. Jamal, M. Bashar, A. Hasan, … Z. A.-… and S. E., and undefined 2018, "Fabrication techniques and morphological analysis of perovskite absorber layer for high-efficiency perovskite solar cell: A review," Elsevier, Accessed: Mar. 05, 2025. [Online]. Available: https://www.sciencedirect.com/science/article/pii/S1364032118306646
10. M. Mattur, N. Nagappan, S. Rath, T. T.-J. of Materiomics, and undefined 2022, "Prediction of nature of band gap of perovskite oxides (ABO3) using a machine learning approach," Elsevier, Accessed: Mar. 05, 2025. [Online]. Available: https://www.sciencedirect.com/science/article/pii/S2352847822000545
11.]N. Bibi, M. U.-M. S. in S. Processing, and undefined 2025, "A theoretical investigation of ABO3 (A= Na and B= Ti, In) perovskites for solar cell and optoelectronic applications," Elsevier, Accessed: Mar. 05, 2025. [Online]. Available: https://www.sciencedirect.com/science/article/pii/S1369800124009430
12. W. Yin, J. Yang, J. Kang, Y. Yan, S. W. M. C. A, and undefined 2015, "Halide perovskite materials for solar cells: a theoretical review," pubs.rsc.org, doi: 10.1039/c0xx00000x.
13. K. Ahmad, M. Khan, H. K.-O. Materials, and undefined 2022, "Simulation and fabrication of all-inorganic antimony halide perovskite-like material based Pb-free

perovskite solar cells," Elsevier, Accessed: Mar. 05, 2025. [Online]. Available: https://www.sciencedirect.com/science/article/pii/S0925346722004086

14. E. Della Gaspera, Y. Peng, Q. Hou, L. Spiccia, U. B.-N. Energy, and undefined 2015, "Ultra-thin high efficiency semitransparent perovskite solar cells," Elsevier, Accessed: Mar. 05, 2025. [Online]. Available: https://www.sciencedirect.com/science/article/pii/S2211285515000877
15. H. Abedini-Ahangarkola, S. Soleimani-Amiri, S. R.-S. Energy, and undefined 2022, "Modeling and numerical simulation of high efficiency perovskite solar cell with three active layers," Elsevier, Accessed: Mar. 05, 2025. [Online]. Available: https://www.sciencedirect.com/science/article/pii/S0038092X22002213
16. C. Liu, W. Li, C. Zhang, Y. Ma, J. Fan, and Y. Mai, "All-Inorganic CsPbI2Br Perovskite Solar Cells with High Efficiency Exceeding 13%," J Am Chem Soc, vol. 140, no. 11, pp. 3825–3828, Mar. 2018, doi: 10.1021/JACS.7B13229.
17. K. Bhojanaa, A. P.-M. C. and Physics, and undefined 2021, "Contribution of interconnection in barium stannate with titania for enhancing photovoltaic performance of dye-sensitized solar cells," Elsevier, Accessed: Mar. 05, 2025. [Online]. Available: https://www.sciencedirect.com/science/article/pii/S0254058421004417
18. N. Kapse, V. Pandit, … V. K.-…-A. Q. J., and undefined 2024, "Antimicrobial activity of ABO3 perovskite nanoparticles (Bnn, Snn, and Bsnn) against E. coli," indianjournals.com, Accessed: Mar. 05, 2025. [Online]. Available: https://www.indianjournals.com/ijor.aspx?target=ijor:bil&volume=21&issue=2&article=042&type=pdf
19. V. K. Kashte, N. N. Kapse, V. A. Pandit, and B. G. Toksha, "A Review on Graphene Oxide-Based Ferrite Nanocomposites for Catalytic Applications," Catalysis Surveys from Asia, Dec. 2024, doi: 10.1007/S10563-024-09434-1.
20. V. Pandit, G. Repe, … J. B.-J. of physics, and undefined 2020, "A review on green synthesis and characterization technique for ferrite nanoparticles and their applications," iopscience.iop.org, Accessed: Mar. 05, 2025. [Online]. Available: https://iopscience.iop.org/article/10.1088/1742-6596/1644/1/012009/meta
21. V. Kashte, V. Pandit, N. Kapse, … D. R.-… of S. and, and undefined 2025, "Effect of Al3+ Doping on the Microstructure and Magnetic Behavior of CoFe2O4 Nanoparticles," SpringerVK Kashte, VA Pandit, NN Kapse, D Rathod, BG TokshaJournal of Superconductivity and Novel Magnetism, 2025•Springer, Accessed: Mar. 05, 2025. [Online]. Available: https://link.springer.com/article/10.1007/s10948-024-06892-6
22. V. Pandit, N. Kapse, … V. K.-J. of M. and, and undefined 2024, "Magnetic Behaviour, and initial permeability of green synthesized Co2+ substituted Ni-Zn ferrite," ElsevierVA Pandit, NN Kapse, VK Kashte, ND ChaudhariJournal of Magnetism and Magnetic Materials, 2024•Elsevier, Accessed: Mar. 05, 2025. [Online]. Available: https://www.sciencedirect.com/science/article/pii/S030488532400475X
23. V. Pandit, K. Sature, … D. T.-…-A. Q. J., and undefined 2022, "Properties of cr doped NI-ZN ferrite nanoparticles synthesized using lemon juice," indianjournals.comVA Pandit, KR Sature, DP Thorat, RA Gaikwad, DM Sonawane, PP Raut, GM DharneBIOINFOLET-A Quarterly Journal of Life Sciences, 2022•indianjournals.com, Accessed: Mar. 05, 2025. [Online]. Available: https://www.indianjournals.com/ijor.aspx?target=ijor:bil&volume=19&issue=2&article=025